

macQsimal	Title Cavity-enhanced GHz field sensor setup	Deliverable Number D7.4
Project Number 820393		Version 1.0

H2020-FETFLAG-2018-2021

macQsimal

Miniature Atomic vapor-Cell Quantum devices for SensIng and Metrology AppLications

Deliverable 7.4

Cavity-enhanced GHz field sensor setup

WP7 – Atomic GHz & THz sensors and vector imagers

Authors: Yongqi Shi, Michael Vogelpohl, Philipp Treutlein (UNIBAS)

Lead participant: UNIBAS

Delivery date: 30.04.2022

Dissemination level: Public

Type: R (Document, Report)



macQsimal	Title Cavity-enhanced GHz field sensor setup	Deliverable Number D7.4
Project Number 820393		Version 1.0

Revision History

Author Name, Partner short name	Description	Date
Yongqi Shi, UNIBAS Michael Vogelpohl, UNIBAS Philipp Treutlein, UNIBAS	Draft	25.04.2022
Rebecca Schmieg, UCPH	Review	29.04.2022
Yongqi Shi, UNIBAS Michael Vogelpohl, UNIBAS Philipp Treutlein, UNIBAS	Final Version	29.04.2022

macQsimul	Title Cavity-enhanced GHz field sensor setup	Deliverable Number D7.4
Project Number 820393		Version 1.0

Abbreviations

cw	Continuous wave
ECDL	External Cavity Diode Laser
EMI	Electromagnetic Interference
GHz	Gigahertz
GSHE	Ground-State Hanle Effect
Hfs	Hyperfine splitting
K	Potassium
MHz	Megahertz
MW	Microwave
ODMR	Optically Detected Magnetic Resonance
PBC	Polarization Beamsplitter Cube
Rb	Rubidium
RBW	Resolution Bandwidth
RF	Radio Frequency
SMA	Sub-Miniature Version A

Partner short names

UCPH	Københavns Universitet, DK (NBI – Niels Bohr Institute)
UNIBAS	Universität Basel, CH

macQsimal	Title Cavity-enhanced GHz field sensor setup	Deliverable Number D7.4
Project Number 820393		Version 1.0

Contents

1 INTRODUCTION AND MOTIVATION 6

2 GHZ FIELD SENSOR SETUP AND OPERATION..... 6

2.1 Measurement scheme..... 6

2.2 Experimental setup..... 7

2.3 Measurement results 8

2.3.1 GHz polarization rotation signal as a function of MW field strength..... 8

2.3.2 Sensitivity..... 10

2.3.3 GHz polarization rotation spectroscopy 11

3 CONCLUSION AND OUTLOOK12

4 REFERENCES13

macQsimal	Title Cavity-enhanced GHz field sensor setup	Deliverable Number D7.4
Project Number 820393		Version 1.0

Executive Summary

This deliverable reports an experimental setup and the operation of a GHz field sensor that uses an atomic vapor cell for direct detection of microwave magnetic fields at GHz frequency. The detector is based on polarization rotation of a detuned laser beam probing an optically-pumped atomic vapor in a buffer gas filled microfabricated vapor cell. The hyperfine coherence, associated with the hyperfine transition between ground states of Rb atoms driven by the microwave field of interest, is oscillating at 6.8 GHz and results in a polarization rotation signal at this frequency. The signal is observed to scale with the amplitude of the applied microwave magnetic field, as expected for coherent driving. Compared to the earlier work [1], background signals are significantly reduced, allowing for a clean detection of the microwave signal with the atoms. The setup is compatible with cavity enhancement of the atom-light interaction to further increase the sensitivity.

macQsimal	Title Cavity-enhanced GHz field sensor setup	Deliverable Number D7.4
Project Number 820393		Version 1.0

1 Introduction and Motivation

Atomic vapor cell based sensors for the detection and imaging of high-frequency electromagnetic fields in the microwave and Terahertz band have seen rapid development in recent years. Different schemes have been used to measure the magnetic component of a microwave field, including time-domain Rabi oscillations [2-3], adiabatic rapid passage [4], and Rabi resonance (atomic candle method) [5]. On the other hand, the electric component of a microwave field can be measured by the induced Autler-Townes splitting of Rydberg transitions in an atomic vapor cell [6-7]. All these methods use light to detect microwave transitions between different energy levels of the atomic ensembles, exploiting different aspects of the atom-light interaction for microwave-to-optical signal conversion [8-9]. The quantum nature of the atoms enables non-invasive [10], calibration-free [10], SI traceable [11], and very sensitive [7] detection of microwave fields. These advantages over traditional methods to detect microwave fields make atomic vapor cells a very promising candidate for future microwave sensing applications, e.g., in the microwave industry or in medical imaging [12-13].

The polarization rotation of an off-resonant laser beam induced by its interaction with a spin-polarized atomic vapor is one important aspect of the atom-light interaction [8-9]. It is frequently employed in atomic magnetometers measuring very weak DC magnetic fields [14-15], and low frequency radio-frequency (RF) magnetic fields [16], with frequencies typically below 1 MHz, resonant with the Zeeman transitions of the atoms. Using advanced techniques such as cavity-enhancement of the atom-light interaction and stroboscopic measurements for quantum back action evasion, Faraday-rotation-based RF magnetometers have been used for quantum enhanced sensing [17-19].

In this report, we describe a setup for direct detection of microwave fields with a ^{87}Rb atomic vapor cell, exploiting the polarization rotation of a far off-resonant probe beam at GHz frequency (6.8 GHz). Compared with the low frequency Faraday rotation associated with the Zeeman coherence generated by RF magnetic fields, the GHz frequency polarization rotation originates from the hyperfine coherence induced by the microwave magnetic field of interest. We measure the GHz polarization rotation signal as a function of microwave (MW) power, demonstrating that it scales linearly with the field strength, as expected for coherent coupling, and use it to measure weak MW magnetic fields. Compared to earlier work [1], our setup achieves a better suppression of background signals from electromagnetic interference, allowing for a clean detection of the microwave signal with the atoms. The detection scheme is also related to parametric frequency conversion in early optical pumping experiments, where the intensity of the pump beam is modulated at MW frequency [20-24]. Our setup is compatible with cavity enhancement of the atom-light interaction and stroboscopic detection for back-action evasion, which could enable quantum enhanced measurements of GHz magnetic field in the future.

2 GHz field sensor setup and operation

In this section, we briefly explain the concept of our measurement scheme, the experimental setup as well as some technical improvement is introduced, and finally we show results of GHz polarization rotation measurements and demonstrate the feasibility of this method for sensing GHz magnetic fields.

2.1 Measurement scheme

A schematic of our setup is shown in Figure 1. At the heart of the setup is an ensemble of ^{87}Rb atoms in an atomic vapor cell. A σ_- polarized pump beam resonant with the $D1$ transition $|F = 2\rangle \rightarrow |F'\rangle$ spin-polarizes the atoms in the $|F = 2\rangle$ hyperfine manifold, pumping the atomic population towards the sublevel $|F = 2, m_F = -2\rangle$. Since the buffer gas (15 mbar N_2 + 18.7 mbar Ar) collisional broadening (1 GHz) is less than the ground state hyperfine splitting (6.8 GHz), the lower hyperfine manifold $|F = 1\rangle$ is much less addressed by the optical pumping beam compared with the $|F = 2\rangle$ manifold. As a result

macQsimal	Title Cavity-enhanced GHz field sensor setup	Deliverable Number D7.4
Project Number 820393		Version 1.0

of the pumping, there are significant population differences between several pairs of sublevels: $|F = 2, m_F = -2\rangle$ and $|F = 1, m_F = -1\rangle$; $|F = 2, m_F = -1\rangle$ and $|F = 1, m_F = -1\rangle$; and so on, representing different hyperfine transitions that can be driven by MW magnetic fields with suitable polarizations. We select the microwave π transition $|F = 1, m_F = -1\rangle \leftrightarrow |F = 2, m_F = -1\rangle$ in the following measurements, since we empirically find that it gives the largest signal (discussed in Section 2.3.3). The MW frequency is set to be on resonance with this transition, taking into account the Zeeman splitting (59.43 kHz) from the applied DC magnetic field and the buffer gas induced frequency shift.

To detect the polarization rotation, we use a separate probe beam, which is 70 GHz red-detuned from the D2 line. The polarization of the probe beam is horizontally linearly polarized (along x direction) before it enters the vapor cell. Since the DC magnetic field is set to be along the z direction, which is also the quantization axis, the input probe can be considered as a superposition of σ_+ and σ_- components. Based on the selection rules and population imbalances, the σ_+ and σ_- component will have different phase shift after going through the vapor cell, which leads to a polarization rotation. In the presence of a continuous wave (cw) MW magnetic field, the hyperfine coherence is oscillating at MW frequency (in the lab frame), generating a frequency component in the polarization rotation signal at the same frequency. We analyse the polarization rotation of the probe beam with a half-wave plate that turns the polarization by 45° before it goes through a polarization beam splitter. For simplicity, only one output port of the polarization beamsplitter cube (PBC) is measured with a fast photodetector of 25 GHz bandwidth¹. The signal is amplified by 35 dB and finally analysed by a microwave spectrum analyser. The resulting signal will be shown and discussed in detail in Section 2.3.

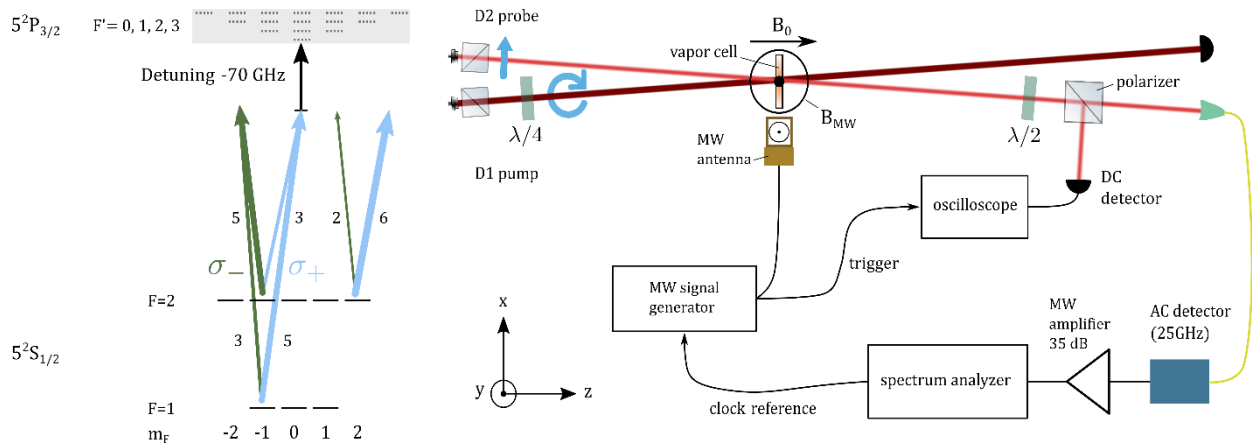


Figure 1: Left: Probe beam transitions and MW transition (the pump beam transition and population distributions are not shown); Right: Measurement scheme and experimental setup.

2.2 Experimental setup

We use a miniaturized atomic vapor cell consisting of a silicon layer with a cavity for the atoms sandwiched between two glass windows, fabricated by anodic bonding in the group of Gaetano Mileti [25]. The cylindrical cavity in the silicon layer has 5 mm in diameter and 2 mm in thickness. The cell is filled with isotopically enriched ^{87}Rb with an abundance of 75%. Nitrogen (15 mbar) and Argon (18.7 mbar) serve as buffer gases to slow down atomic motion in order to increase the spin relaxation time of the atoms. Nitrogen also quenches the spontaneous fluorescence to prevent radiation trapping.

¹ We note that one could alternatively detect both outputs of the PBC and mix down both microwave signals to perform a low frequency homodyne measurement.

macQsimal	Title Cavity-enhanced GHz field sensor setup	Deliverable Number D7.4
Project Number 820393		Version 1.0

The cell is heated and temperature stabilized to $90 \pm 0.1^\circ\text{C}$ by an oven (not shown), so the atom density is approximately $2.3 \times 10^{12}\text{cm}^{-3}$, which is calculated from vapor-pressure model [26].

The cell together with oven is placed inside a cylinder shaped single-layer mu-metal shield (with a shielding factor of nearly 100). By manipulating the currents of an integrated three-axis Helmholtz coil system, we can further reduce the remnant DC magnetic field, using the ground state Hanle effect (GSHE) method [27-28]. The eventual residual field in the xy-plane is less than $0.05 \mu\text{T}$. In the main experiment, we apply a moderate DC field ($8.49 \mu\text{T}$) along z-direction as a guiding field for the spin polarization. For calibrating the z-direction coil, we use optically detected magnetic resonance (ODMR) [27] of the atomic vapor by applying an RF field in the x-direction and scanning the DC field in z-direction. The ODMR peaks can be measured together with the GSHE peak. Using the gyromagnetic ratio of ^{87}Rb (7 Hz/nT), the calibration constant of the z-direction Helmholtz coil is found to be 414 nT/mA , and a similar calibration constant of 413 nT/mA is found using a commercial fluxgate magnetometer at the same position.

The lasers used in the experiment are both home-made interference-filter-based external cavity diode lasers (ECDL) [29]. The unique cat-eye feature of this type of ECDL provides better frequency stability from mechanical vibration compared with Littrow scheme ECDLs. The frequency fluctuation of the free-running laser is around 20 MHz in a measurement time window of several minutes, which is good enough for getting the preliminary signal. Further improvements should be made to stabilize both the frequency and power of the lasers to increase the sensitivity.

We shorted a Sub-Miniature Version A (SMA) jack to serve as a microwave rectangular loop antenna. By aligning the loop parallel to the xz-plane a few millimetres away from the cell, we can generate mostly linearly polarized microwave magnetic fields in the vertical direction (y-direction) in the cell region (the sphere on the schematic). Since the quantization axis of the whole system is defined by the DC magnetic field ($\vec{B}_{\text{DC}} = B_{\text{DC}}\hat{z} = 8.49 \mu\text{T}\hat{z}$) along the z-direction, the microwave magnetic field can be decomposed into left- and right-handed circularly polarized components, and induces mostly σ_+ and σ_- microwave transitions. The homogeneity of the MW field turned out to be sufficient to see the signal, while in future experiments, a tailored antenna or waveguide is expected to define a more homogeneous and a more confined field so as to increase the sensitivity further. The MW is generated by a signal generator (Rohde & Schwarz SMB 100A). A directional coupler (Mini-Circuits ZCDC20-06263-S+) and a MW circulator (Ditom DMC6018) are connected between the generator and the antenna to protect the former from reflections from the antenna (shorted jack).

The transmitted probe beam is coupled to a 4-meter-long single-mode fiber and guided to a high frequency photodetector (25 GHz bandwidth, DXM25CF) which is placed far away from the MW antenna, to avoid capturing the MW signals directly from the antenna. The MW component of the optical signal is then amplified by a MW amplifier (Mini-Circuits ZVE-3W-183+) by 35 dB and analysed by a spectrum analyser (Rohde & Schwarz FSV3013) in different conditions.

2.3 Measurement results

We now present measurements of the GHz polarization rotation of the light induced by the microwave driven atomic vapor, in different experimental conditions: 1) the signals as a function of MW field strength at a fixed frequency; 2) comparison between signals and spurious peaks transmitted through the air; 3) spectra of the GHz signal amplitude when scanning the frequency of the MW field.

2.3.1 GHz polarization rotation signal as a function of MW field strength

First, we fix the frequency of the cw MW signal from the signal generator to be on resonance with $|F = 1, m_F = -1\rangle \leftrightarrow |F = 2, m_F = -1\rangle$ ($f_{\text{MW}} = 6.834569080 \text{ GHz}$, considering the clock shift due to the buffer gas and Zeeman splitting in the DC field of $8.49 \mu\text{T}$) and set the MW power to different

macQsimal	Title Cavity-enhanced GHz field sensor setup	Deliverable Number D7.4
Project Number 820393		Version 1.0

values. The resonant pump beam has a power of 0.4 mW and the 70 GHz detuned probe beam has a power of 18 mW. We set the centre frequency of the spectrum analyser to be the same as the applied MW field and the frequency span to 100 Hz, with a resolution bandwidth (RBW) of 1 Hz. The RBW is always set to be 1 Hz, except for Figure 5. We then record the signals from the spectrum analyser for different input MW powers. The results are shown in Figure 2 in linear voltage scaling.

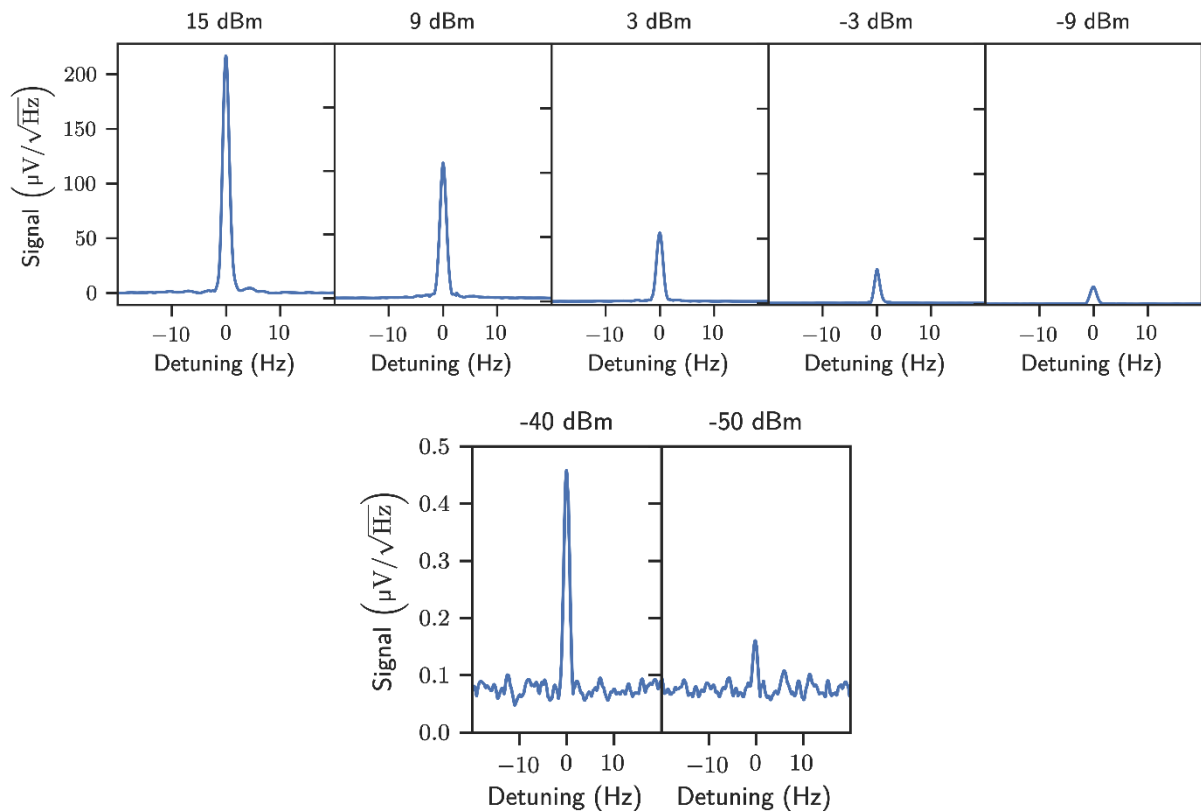


Figure 2: Polarization rotation signal at $f_{MW} = 6.834569080$ GHz for different applied MW powers.

In Figure 3 we plot the peak signal amplitude (integrated in 1Hz bandwidth) as a function of the square root of MW power ($\sqrt{P_{MW}(\text{mW})} \propto B_{MW}$) and observe a linear scaling. This is consistent with coherent driving, i.e., the polarization rotation signal is proportional to the amplitude of the MW magnetic field through the Rabi frequency (Ω_{Rabi}) of the hyperfine transition (Figure 3). The data is fit with the function

$$\text{Signal}(\mu\text{V}) = m\sqrt{P_{MW}(\text{mW})}$$

with the fit returning $m_{\text{fit}} = 38.3(2)$. In these measurements, all other conditions remain the same except for the MW power.

macQsimal	Title Cavity-enhanced GHz field sensor setup	Deliverable Number D7.4
Project Number 820393		Version 1.0

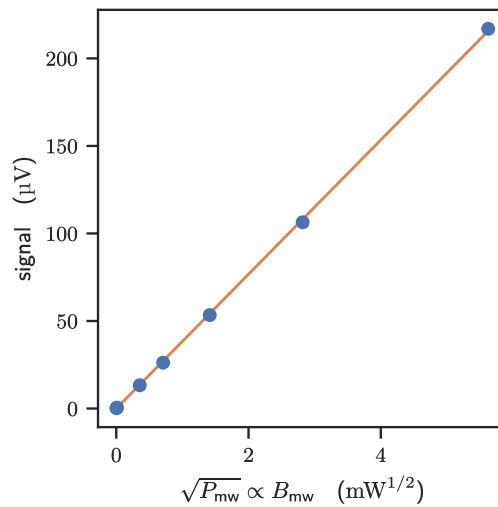


Figure 3: GHz polarization rotation signals as a function of $\sqrt{P_{MW}(\text{mW})} \propto B_{MW}$.

2.3.2 Sensitivity

In order to evaluate the sensitivity of this method for microwave field detection, we first determine the minimum detectable signal in the same configuration as in the Section 2.3.1.

If the MW is set to the maximum available power (+15 dBm), we measured the polarization rotation signal peak to be around 200 μV (red peak in Figure 4). For such high MW powers, we still see a MW peak on the spectrum analyzer even if the pump and probe lasers are blocked (blue peak in Figure 4), indicating that the MW field is also directly transmitted from the antenna through air to the detector (Electromagnetic Interference (EMI) problem). It seems to be mainly coupled into the detection path through insufficient shielding of the ultrafast photodetector. By using a 4m long single mode fibre between cell and detector, moving the detector far away and covering it with metal foams, this spurious signal is minimized to be two orders of magnitude smaller than the polarization rotation signal induced by the atoms.

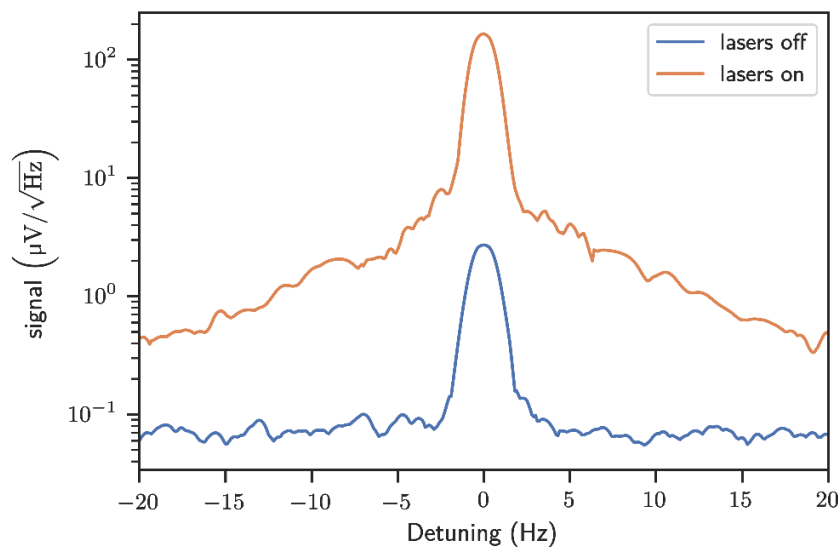


Figure 4: GHz polarization rotation signal when lasers are on (red peak) and air transmitted spurious signal when lasers are off (blue peak); MW power is +15 dBm in both cases.

macQsimal	Title Cavity-enhanced GHz field sensor setup	Deliverable Number D7.4
Project Number 820393		Version 1.0

If we now set the MW input power to -50 dBm, we still see a polarization rotation signal, with no visible background peak if the lasers are off, see Figure 5. The polarization rotation signal peak is $0.15 \mu\text{V}$ and the noise floor is approximately $0.08 \mu\text{V}/\sqrt{\text{Hz}}$, so the signal to noise ratio (SNR) is around 1.9 in a 1 Hz bandwidth. The noise floor corresponds to approx. -130 dBm/Hz (with 50 ohms impedance), while the sensitivity of the spectrum analyser at this frequency is -145 dBm/Hz [31]. Note that we also use a MW high power amplifier with a gain of 35 dB before the spectrum analyser. After calibration measurement, we find that this amplifier increases the noise floor at this frequency by around 13 dB/Hz while the photon shot noise (as well as the technical noise from the ultrafast detector) at this frequency is around 1 dB/Hz. The detected MW signal power (-50 dBm) is already lower than the value demonstrated in [1], due to the elimination of the air transmitted EMI signal in our case. Meanwhile, the experimental conditions as well as the antenna structures are different and we use a different MW transition. To further increase the sensitivity, the optical pump and probe powers, the polarizations, the probe detuning as well as the cell parameters could be optimized.

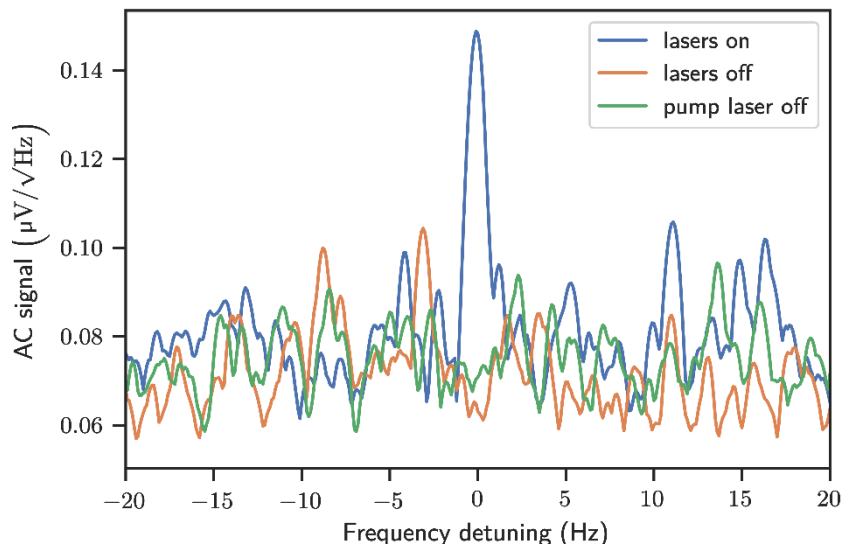


Figure 5: GHz polarization rotation signal when lasers are on (blue peak) and the noise floor when both lasers are off (red curve) or only the pump laser is off (green curve); MW power is -50 dBm in all cases.

2.3.3 GHz polarization rotation spectroscopy

In order to investigate the underlying physics of the GHz polarization rotation signal, we performed an additional measurement where we scan the MW signal generator in a slow step mode. The step frequency is 1 kHz and there are 400 steps, so the bandwidth to be measured is 400 kHz around the clock frequency. The step time is 100 ms so one run costs around 40 s. On the spectrum analyzer side, we set RBW = 100 Hz, sweep time = 42 ms, frequency span = 600 kHz around the same center frequency as signal generator, and the trace mode is set to be “MaxHold”. With this method, the peak signal amplitudes of GHz polarization rotation signal at different detuning can be recorded. The resulting GHz polarization rotation spectrum (one run of step-mode scanning) is shown in Figure 5: the blue curve is measured with a MW power of +15 dBm and the red curve with -15 dBm, note that only the central data with 400 kHz bandwidth is shown. Each point is recorded with at least 2 times average. Three prominent peaks in both cases represent the three π transition between the two hyperfine manifolds. This is surprising since the orientation of the loop antenna is such that we would have expected stronger σ_+ and σ_- transitions than π transitions driven by the microwave field. Since the loop antenna is made by shorting the signal and ground pins of a SMA jack, there are additional metallic structures (for example the other unsoldered ground pins) nearby, which could distort the microwave

macQsimal	Title Cavity-enhanced GHz field sensor setup	Deliverable Number D7.4
Project Number 820393		Version 1.0

field. Another interesting feature is that the σ_- transition between the two stretched states ($|F = 1, m_F = -1\rangle \leftrightarrow |F = 2, m_F = -2\rangle$) is hard to see. It remains unclear at this stage whether this is due to much smaller population imbalance of these two sublevels. The spectroscopy also shows some asymmetric broadening of the peaks. Further analysis is necessary to fully understand the observed spectra, which will also guide further optimizations of the microwave detector.

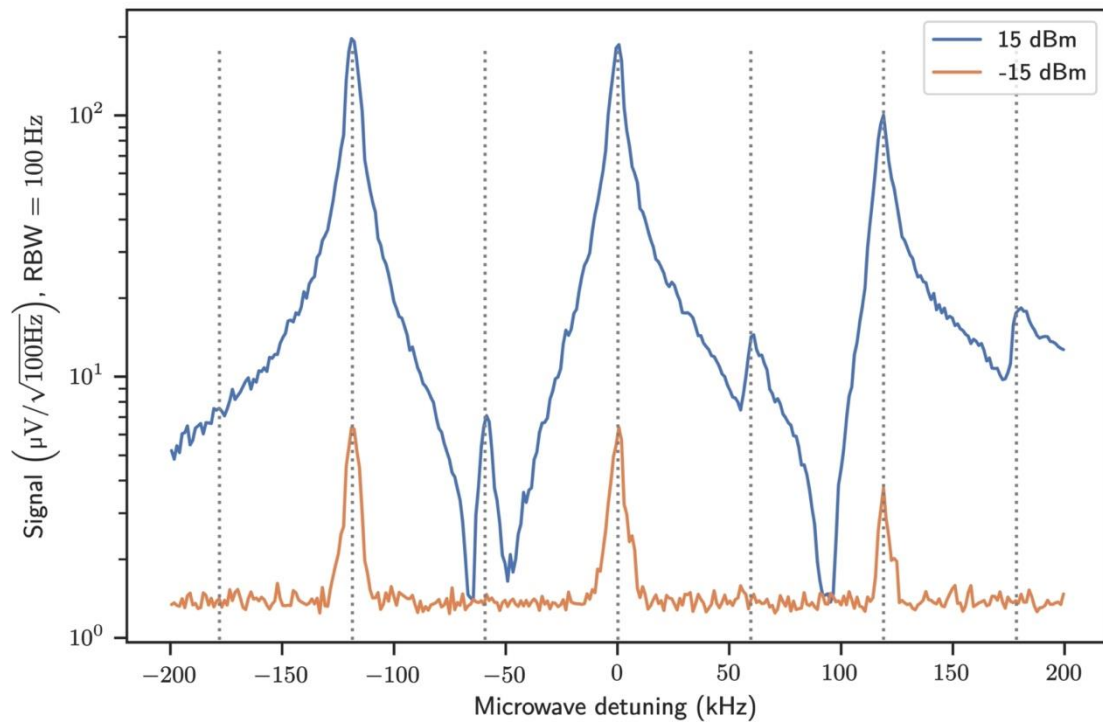


Figure 6: GHz polarization rotation spectroscopy, showing the signal amplitude measured when scanning the MW frequency (RBW = 100 Hz). Blue: MW power = +15 dBm; Red: MW power = +15 dBm.

3 Conclusion and outlook

We have built a setup for direct detection of a GHz magnetic field with an atomic vapor cell, employing the polarization rotation of the light induced by the atomic hyperfine coherences for microwave-to-optical conversion. We have confirmed that the signal amplitude is proportional to the amplitude of the MW magnetic field, i.e., the Rabi frequency of the microwave transition between the two ground-state hyperfine manifolds. The minimum detectable MW power in the current setup is around -50 dBm. In the future, the setup can be integrated with a cavity to enhance the light-matter interaction and serve as a platform to explore quantum enhancement strategies in the measurement of weak microwave fields.

macQsimal	Title Cavity-enhanced GHz field sensor setup	Deliverable Number D7.4
Project Number 820393		Version 1.0

4 References

- [1] Gerginov, Vladislav, et al. "An atomic sensor for direct detection of weak microwave signals." *IEEE Transactions on Microwave Theory and Techniques* 67.8 (2019): 3485-3493.
- [2] Böhi, Pascal, and Philipp Treutlein. "Simple microwave field imaging technique using hot atomic vapor cells." *Applied Physics Letters* 101.18 (2012): 181107.
- [3] Horsley, Andrew, and Philipp Treutlein. "Frequency-tunable microwave field detection in an atomic vapor cell." *Applied Physics Letters* 108.21 (2016): 211102.
- [4] Frueholz, R. P., and J. C. Camparo. "Microwave field strength measurement in a rubidium clock cavity via adiabatic rapid passage." *Journal of Applied Physics* 57.3 (1985): 704-708.
- [5] Sun, Fuyu, et al. "Measuring microwave cavity response using atomic Rabi resonances." *Applied Physics Letters* 111.5 (2017): 051103.
- [6] Sedlacek, Jonathon A., et al. "Microwave electrometry with Rydberg atoms in a vapour cell using bright atomic resonances." *Nature Physics* 8.11 (2012): 819-824.
- [7] Jing, Mingyong, et al. "Atomic superheterodyne receiver based on microwave-dressed Rydberg spectroscopy." *Nature Physics* 16.9 (2020): 911-915.
- [8] Happer, William. "Optical pumping." *Reviews of Modern Physics* 44.2 (1972): 169.
- [9] Hammerer, Klemens, Anders S. Sørensen, and Eugene S. Polzik. "Quantum interface between light and atomic ensembles." *Reviews of Modern Physics* 82.2 (2010): 1041.
- [10] Horsley, Andrew, Guan-Xiang Du, and Philipp Treutlein. "Widefield microwave imaging in alkali vapor cells with sub-100 μm resolution." *New Journal of Physics* 17.11 (2015): 112002.
- [11] Paulusse, David C., Nelson L. Rowell, and Alain Michaud. "Accuracy of an atomic microwave power standard." *IEEE Transactions on Instrumentation and Measurement* 54.2 (2005): 692-695.
- [12] Baili, Ghaya, et al. "Quantum-based metrology for timing, navigation and RF spectrum analysis." *European Defence Agency, Quantum Technologies in Optronics: Optronics Workshop Proceedings*. 2019.
- [13] Mathur, Monika, et al. "Microwave Imaging Breast Cancer Detection Techniques: A Brief Review." *Optical and Wireless Technologies* (2022): 203-210.
- [14] Budker, Dmitry, et al. "Resonant nonlinear magneto-optical effects in atoms." *Reviews of modern physics* 74.4 (2002): 1153.
- [15] Dang, H. B., Adam C. Maloof, and Michael V. Romalis. "Ultrahigh sensitivity magnetic field and magnetization measurements with an atomic magnetometer." *Applied Physics Letters* 97.15 (2010): 151110.
- [16] Savukov, Igor M., et al. "Tunable atomic magnetometer for detection of radio-frequency magnetic fields." *Physical review letters* 95.6 (2005): 063004.
- [17] Wasilewski, Wojciech, et al. "Quantum noise limited and entanglement-assisted magnetometry." *Physical Review Letters* 104.13 (2010): 133601.
- [18] Vasilakis, Georgios, et al. "Generation of a squeezed state of an oscillator by stroboscopic back-action-evading measurement." *Nature Physics* 11.5 (2015): 389-392.
- [19] Bao, Han, et al. "Spin squeezing of 1011 atoms by prediction and retrodiction measurements." *Nature* 581.7807 (2020): 159-163.

macQsimal	Title Cavity-enhanced GHz field sensor setup	Deliverable Number D7.4
Project Number 820393		Version 1.0

[20] Firester, Arthur H., and Thomas R. Carver. "Light Modulation at the Ground-State Hyperfine-Separation Frequency of Potassium." *Physical Review Letters* 17.18 (1966): 947.

[21] Firester, Arthur H., and Thomas R. Carver. "Intensity Modulation of Transmitted Light at the Ground-State Hyperfine Frequency of K 39." *Physical Review* 164.1 (1967): 76.

[22] Mathur, B. S., et al. "Microwave Light Modulation by an Optically Pumped Rb 87 Vapor." *Physical Review Letters* 21.15 (1968): 1035.

[23] Tang, H., and W. Happer. "Parametric frequency conversion of resonance radiation in optically pumped rubidium-87 vapor." *Physical Review Letters* 24.11 (1970): 551.

[24] Tang, Henry. "Parametric Frequency Conversion of Resonance Radiation in Optically Pumped Rb 87 Vapor." *Physical Review A* 7.6 (1973): 2010.

[25] Pellaton, Matthieu, et al. "Study of laser-pumped double-resonance clock signals using a microfabricated cell." *Physica Scripta* 2012.T149 (2012): 014013.

[26] Daniel A. Steck, "Rubidium 87 D Line Data," available online at <http://steck.us/alkalidata> (revision 2.2.2, 9 July 2021).

[27] Castagna, Natasha, and Antoine Weis. "Measurement of longitudinal and transverse spin relaxation rates using the ground-state Hanle effect." *Physical Review A* 84.5 (2011): 053421.

[28] Breschi, Evelina, and Antoine Weis. "Ground-state Hanle effect based on atomic alignment." *Physical Review A* 86.5 (2012): 053427.

[29] Baillard, X., et al. "Interference-filter-stabilized external-cavity diode lasers." *Optics Communications* 266.2 (2006): 609-613.

[30] Rohde & Schwarz, "R&S FSV3000 Signal and Spectrum Analyzer - Specifications", Version 09.00, March 2022, available online at https://scdn.rohde-schwarz.com/ur/pws/dl_downloads/dl_common_library/dl_brochures_and_datasheets/pdf_1/FSV3000_dat-sw_en_5216-1334-22_v0900.pdf

[31] Happer, W., and B. S. Mathur. "Effective operator formalism in optical pumping." *Physical Review* 163.1 (1967): 12.

[32] Mathur, B. S., H. Y. Tang, and W. Happer. "Light propagation in optically pumped alkali vapors." *Physical Review A* 2.3 (1970): 648.